EXPERIMENTAL METHODS FOR GEOLOGICAL REMOTE SENSING

by

Robert K. Vincent
The University of Michigan
Willow Run Laboratories
Ann Arbor, Michigan

INTRODUCTION

At Willow Run Laboratories in 1970, under NASA Contract 9-9784, a two channel analog ratio technique in the thermal IR wavelength region for mapping gross compositional variations in silicate rocks was developed which successfully produced automatic ratio recognition maps of quartz sand and sandstone near the Mill Creek, Oklahoma sand quarry. In the report which describes that effort [1], a three channel IR technique was hypothesized for a more refined version of this ratio method, whereby the third channel is used for correction of temperature variations across the target scene. It was also hypothesized that the resulting temperature-corrected ratios would be at least crudely correlated with SiO_2 content of the geological targets encountered.

During 1971, the state-of-the-art of geological remote sensing was further advanced by the processing of data from an aircraft flight over Pisgah Crater, California. There are four major results from the Pisgah Crater data. First, the two-channel thermal IR analog ratio method from last year has been successfully used to map relative differences among various silicate rock types. Secondly, the three-channel thermal IR technique, hypothesized last year, has been implemented successfully to make digital temperature-corrected ratio maps which are more sensitive than the two-channel ratio maps to true compositional variations in geological targets. Thirdly, a new technique involving the ratio of radiances in visible green to reflective IR channels has been theorized and qualitatively tested for the purpose of mapping variations in iron oxides on the surfaces of exposed rocks.

The Pisgah Crater area in San Bernardino County was chosen as a test site for three reasons: there are many silicate rock types in close proximity, the semiarrid terrain is very sparsely vegetated, and considerable ground truth data was already available about the area from other reports and geologic maps [2,3]. The flight took place on 30 October 1971 between 0800 (approximately 1 hour after sunrise) and 0840 hours, local time, at above-ground altitudes of 500 ft and 3000 ft. Only the 3000 ft data was processed through to the final stages because of monetary limitations. The morning was clear, with relative humidity less than 25% and a ground-level air temperature of approximately 5°C. This time of day was chosen because

temperature variations across the scene due to compositional effects (albedo, thermal conductivity, etc.) were small, yet enough solar illumination was available for visible and reflective IR data collection.

Dr. Larry C. Rowan, a U. S. Geological Survey geologist from the Regional Geophysics Office in Denver, and Ben Drake, a geology Ph.D. candidate at The University of Michigan, greatly assisted the author in field checking these images.

DESCRIPTION OF APPARATUS AND METHOD OF ANALYSIS

The data were collected by The University of Michigan multispectral scanner (4) and a Honeywell two-element Hg:Cd:Te detector filtered (5) to the approximate 10% cutoff points of 8.2 μm - 10.9 μm and 9.4 μm - 12.1 μm, which will be called channels 1 and 2, respectively, aboard the University's C-47 aircraft. The two methods of analysis for the thermal IR data are described in references 1 and 5. Briefly, in the first method, the ratio of radiances in channel 1 to channel 2 was made the "signal" to the University's analog computer. The resulting "ratio images" are bright where this R_{12} ratio is high and dark where R_{12} is low. Silicate rocks display various spectral emittance minima in the 8 μm - 14 μm region, caused by reststrahlen bands (molecular vibrational modes). Generally speaking, felsic (silica-rich) rocks tend to have spectral emittance minima at shorter wavelengths than mafic (silica-poor) rocks. Hence, there is a tendency for the R_{12} ratio to be lower for felsic rocks (dark in the ratio image) than for mafic rocks (bright in the ratio image).

The second thermal IR method involves the correction of R_{12} for temperature variations across the scene. The spectral emittance of the geologic target in a channel 3 (11.4 μm - 14.4 μm at 15% points) is assumed to be a constant value for all silicates, which is a reasonably good assumption in that wavelength region. From the channel 3 radiance, the rock temperature is determined (within 5°K), and a ratio correction factor, R_g, is calculated. The R_{12} ratio is then corrected for temperature variations across the scene to yield the temperature-corrected ratio

$$R = R_g R_{12} \tag{1}$$

This three-channel scheme is done digitally. Laboratory emittance spectra and a theoretical atmospheric model are then used to calculate expected R ratios for various rock types. The measured values of R from the scanner data can be compared with these theoretical values to determine broad classifications of rock type. A simpler two-channel scheme for temperature correction, which has proved qualitatively successful, will be implemented quantitatively during the coming year.

The method for the visible-reflective IR ratio images involves a simple ratio of radiances in channel 5 (0.50 μm - 0.52 μm) to channel 7 (0.74

μm - 0.85 μm). Electronic transitions of iron oxides produce a relatively large rise in spectral reflectance from 0.5 μm to .80 μm, compared with lesser or no rise in spectral reflectance over the same spectral region for felsic rocks, and with a drop in reflectance for unoxidized mafic rocks. Thus, generally speaking, iron oxides appear dark, felsic rocks appear a medium gray tone, and unoxidized mafic rocks appear bright on the R_{57} ratio image.

RESULTS AND DISCUSSION

A demonstration of the two-channel IR ratio method is given in figure 1, which shows from top to bottom the analog images of channel 1 (8.2 μm - 10.9 μm), channel 2 (9.4 μm - 12.1 μm), and R_{12} (the ratio of radiances in the two channels) for section 2A of the Pisgah data. This is a region approximately 5 miles south-southeast of Pisgah Crater. North is to the top of the images. The ratio image shows emittance variations which are indicative of rock type differences. The felsic mountains (D) and alluvium (A) appear darker than the mafic lava (LA), and the playa material is contrasted sharply against the alluvium. The topographically higher dacitic mountains (D) are warmer than other parts of the scene, which makes the ratio for that region higher than it should be on the sole basis of reststrahlen position. The patchy appearance of the playa is primarily caused by emittance variations, because the gray level of the single channel images are almost uniform across the floor of Lavic Lake, of which this is a part. The most important fact about this figure, however, is that felsic and mafic lithological units are clearly discriminated in the ratio image.

The three-channel IR technique corrects the R_{12} ratio for temperature variations across the scene via equation (1). It is demonstrated by the digital ratio map in figure 2, which includes almost all of the region shown in figure 1. The ratio R from equation (1) is divided into the following 5 levels:

Level 1	$R \leq .969$
Level 2	$.969 < R \leq .973$
Level 3	$.973 < R \leq .981$
Level 4	$.981 < R \leq .992$
Level 5	$.992 < R$

The lowest recorded R in level 1 is .941 and the highest level recorded level 5 is 1.024. These values for R can be compared directly with the graph in figure 3, which plots R versus $\%SiO_2$ as calculated from laboratory rock emittance spectra of Lyon [6] and an atmospheric model of Anding, et. al. [7]. Levels 1 and 2 are primarily felsic (acidic) silicates and levels 4 and 5 are primarily mafic (basic) silicates. A graybody with constant emittance $\varepsilon = 0.94$ throughout the 7 μm - 14 μm region would yield a ratio value of R = 0.975, which would appear in level 3, along with some of the

intermediate rocks. Graybodies of that type can be distinguished from silicates by ratioing the sum of radiances in channels 1 and 2 to the radiance in channel 3 for the purpose of determining the presence or absence of reststrahlen bands, which was not done here. More and different ranges in R could have been printed, but these ranges and symbols were chosen for printing because they produced a more pleasing figure for demonstration purposes. The estimated error in R is ± .007.

The primary effect of the temperature-correction can be seen in a comparison of R for dacitic mountains (D) with R for the alluvium (A) in figures 1 and 2. Figure 1, which is not temperature-corrected, shows the alluvium as having a lower R_{12} ratio (darker in the R_{12} ratio image) than the adjacent dacitic mountains, even though the alluvium has a chemical composition similar to the mountains (the former consists primarily of rock fragments from the latter). However, the mountains, which are topographically higher, were warmer than the alluvium at this time of morning (see the single channel images of figure 1), which biased the R_{12} ratio toward a higher value in the mountains. Figure 2, on the other hand, shows nearly equal values for R, the temperature-corrected ratio, in the alluvium and in the mountains. This is a good indication that the temperature corrections have been successful.

As a more stringent test of the quantitative accuracy of this method, the ratios of the dacite and plagioclase basalt samples of Lyon, plotted as data points in figure 3, can be compared with ratios for the dacitic mountains (D) (also for the dacitic fragments in the alluvium) and basalts of the Sunshine lava flows (LA) in figure 2. Lyon's dacite yields a theoretical ratio of R = .947, which falls into level 1, a ratio frequently measured in the mountain (D) and alluvium (A) regions of figure 2. Lyon's plagioclase basalt yields a ratio of R = 1.015, which falls into level 5, a commonly measured level in the Sunshine basalt flows (LA) of figure 2. Therefore, the laboratory and scanner data quantitatively agree within reasonable limits (perhaps as small as the estimated ± .007 error in R).

To demonstrate the third ratio technique, ratio images of radiances in the visible green, channel 5 (0.50 μm - 0.52 μm), to reflective IR channel 7 (0.74 μm - 0.85 μm) were processed in a manner similar to the two-channel thermal ratio method discussed above, for approximately the same areas as shown in figures 1 and 2. Figure 4 shows, from top to bottom, analog scanner images of channel 5, channel 7, and the ratio R_{57}. The ratio image shows gray level variations unlike the single channel images. Theoretically, iron oxide will appear dark in the ratio image. The two eruptive phases (labeled 1 and 2) of Sunshine lava display various shades of gray, which are darker than the alluvium (A) on the west side. The younger phase 2 Sunshine lava appears darker in the ratio image than the older phase 1 lava. The greater presence of calcium carbonate on joint planes and in local minor depressions on the phase 1 Sunshine lava accounts, in part, for the lighter color of this unit in the single channel images. This may also partly account for the slightly brighter gray level

in the ratio image.

The alluvial deposits (A) on either side of the Sunshine lava appear quite different in the ratio image. It is probable that the drainage patterns carry more ferric oxides from the Pisgah and Sunshine lava flows to the eastern alluvium (surrounded by basalt) than to the western alluvium (basalt only on one side). This would explain the darker gray level of the eastern deposits in the ratio image. However, the playa and alluvium east of the Sunshine flows appear to have similar spectral properties in these two channels of information, as evidenced by similar gray levels in the ratio image, which may indicate almost equal amounts of surficial ferric oxide in or on both types of material.

Probably the most significant features in the ratio image of figure 4, however, are the dark linear regions in the dacitic mountains on the left side of the image. The two prominent, dark, linear features running northwest to southeast are andesitic dikes in the predominantly dacitic mountain range. The longer dark feature, north of the alluvium inlet, is shown as an andesite dike on T. W. Dibblee's geologic map of the area [8]. The shorter dark feature is an andesitic dike which cuts across the dacitic peninsula on the southern border of the alluvium inlet. This short dike, which is not on Dibblee's map, may be a slightly offset continuation of the more prominent, longer dike. If so, there may be a west-to-east fault below the alluvium in the inlet. The andesitic dikes appear rusty brown to the naked eye of a field geologist on the ground, and, if not in shadow, are easily recognized by ground observers. However, the dikes do not show up well in the single channel images. Contrarily, the ratio image produces excellent contrast between oxidized surfaces of andesite and the surrounding dacite, whether in shadow or bright solar illumination. Finally, the small dark spot at the top of the ratio image on the mountain-alluvium border is a darkly weathered biotite quartz monzonite outcropping that shows up equally well in the ratio or single-channel images.

Generally speaking, acidic (felsic) rocks should contain less ferric oxide than basic (mafic) rocks, because the latter have more iron available for oxidation. Thus, there should be some correlation between R_{12} and R_{57} with respect to silicate rock type. This implies that, low R_{12} and high R_{57} indicate acidic silicates, whereas high R_{12} and low R_{57} indicate basic silicates. Although desert varnish (ferric oxides) can cover any type of rock, it does not seem to prevent the acidic rocks from appearing brighter than basic rocks in the R_{57} ratio of figure 4, except for cases where the felsic rocks contain appreciable amounts of biotite (biotite quartz monzonite in figure 4). The weathered andesite in the dikes of figure 4 is an intermediate rock with relatively high iron content; hence, it has a higher Fe_2O_3 content and appears dark in the R_{57} ratio image, even though it is not bright in the R_{12} image of figure 1.

There are several indications in the Pisgah data that the thermal infrared R_{12} ratio is not very affected by the amount of ferric oxides on

the rock surfaces. For instance, R_{57} variations within Pisgah lava flows (not shown) are not accompanied by similar variations in R_{12}. Laboratory tests are needed to confirm or deny this hypothesis. However, the iron oxide reststrahlen bands occur near 20 μm and greater, which hints that they may be relatively transparent in the silicate reststrahlen region between 8 μm and 12 μm.

CONCLUSIONS

During the past year a 2-channel IR technique for discrimination among silicate rocks was tested for a second time, a three-channel IR method was tested for the first time, and a new visible-reflective IR ratio method was hypothesized and qualitatively tested for iron-oxide recognition. Both the two-channel and three-channel IR ratios methods were capable of discriminating felsic from mafic rock types near Pisgah Crater, California. The three-channel ratio values measured by the scanner were found to agree, within reasonable limits, with the values of R calculated from laboratory data. The capability of the three-channel method to obtain absolute ratios is accompanied by a costly processing routine. The two-channel technique is superior for low thermal contrast scenes ($\Delta T \leq 5°C$) about which some ground truth is available because of its speed and economy ($3400 for data processing of the first 150 data-miles and $750 for each additional 150 data-mile set; this does not include data collection costs).

The reflective channel ratio method was found capable of enhancing the contrast of iron oxides in the presence of unoxidized or iron-deficient rock surfaces. Photographic IR methods can duplicate some of these visible-reflective IR ratio results [9,10] with less image distortion and lower cost. However, this scanner ratio technique (which costs the same as the 2-channel thermal ratio processing) is superior for suppressing shadowing and atmospheric effects.

All three techniques can be useful for geologic mapping. For example, the thermal ratio method should assist in the mapping of volcanic ash flows, which are sometimes indistinguishable to the naked eye from sedimentary material, and glacial tills, which can vary significantly in SiO_2 content. Similarly, the visible-reflective IR ratio should be useful in the exploration for gossans or other iron and nickel ore bodies, as well as for the mapping of iron-rich (lateritic) soils. These and other applications can be tested with esiting equipment and computer software.

REFERENCES

1. R. K. Vincent, R. Horvath, F. Thomson, and E. Work, Remote Sensing Data-Analysis Projects Associated with the NASA Earth Resources Spectral Information System, The Univ. of Mich. Tech. Report 3165-26-T, NASA Contract NAS9-9784, Ann Arbor, Michigan, (1971).

2. T. W. Dibblee, Jr., U.S.G.S., Misc. Geol. Inv. Map I-472 (1966).

3. S. J. Grawarecki, NASA Earth Resources Aircraft Program Status Review, 1, 10-1(1968).

4. L. M. Larsen and P. G. Hasell, Jr., Calibration of an Airborne Multispectral Optical Sensor, The Univ. of Mich. Report No. 6400-137-T, Contract DA 28-043-AMC-00013(E), AD 842419, Ann Arbor, Michigan, (1968).

5. R. K. Vincent, Rock-Type Discrimination from Ratio Images of Pisgah Crater, California Test Site, The Univ. of Mich. Report No. 31650-77-T, Contract NAS9-9784, Ann Arbor, Michigan,(1972).

6. R. J. P. Lyon, Evaluation of Infrared Spectrophotometry for Compositional Analysis of Lunar and Planetary Soils: Rough and Powdered Surfaces, Final Report - Part II under NASA Contract NASr-49(04), Stanford Research Institute, Menlo Park, California, (1964).

7. D. Anding, R. Kauth, and R. Turner, Atmospheric Effects on Infrared Multispectral Sensing of Sea Temperature from Space, The Univ. of Mich. Report 2676-5-P, Ann Arbor, Michigan, (1970).

8. T. W. Dibblee, Jr., Op. Cit.

9. L. Rowan and R. K. Vincent, Abstracts, Annual Meeting of the Geological Society of America, Washington, D. C., p. 739, (1971).

10. R. K. Vincent, Op. Cit.

FIGURE CAPTIONS

FIGURE 1: Analog Infrared images of flightline 2 section A of a west-east flight about 5 miles south of Pisgah Crater. North is toward the top. Channel 1, channel 2, and the R_{12} ratio image are at top, middle, and bottom, respectively. From left to right are dacitic mountains (D), alluvium (A), Sunshine lava flows (LA), alluvium (A), playa material (P) of Lavic Lake, and Pisgah lava (LA) of phase 1.

FIGURE 2: Temperature-corrected digital recognition map of silicate rocks for most of flight line 2, section A (including most of the area covered in figure 1) about 5 miles south of Pisgah Crater. North is to the top. The top and bottom maps are contiguous. Felsic rocks (high $\%SiO_2$) appear yellow and mafic rocks (low $\%SiO_2$) appear blue.

FIGURE 3: Temperature-corrected ratio R versus %SiO2 for 25 rock samples of Lyon [6].

FIGURE 4: Analog visible and reflective IR images of flight line 2 section A of a west-east flight about 5 miles south of Pisgah Crater (same area as in figures 1 and 2). North is toward the top. Channel 5, channel 7, and R_{57} ratio are at top, middle and bottom, respectively. From left to right are dacitic mountains (D) with dark (low ratio) andesitic dikes, alluvium (A), Sunshine lava (LA) of two eruptive phases, alluvium (A), playa material (P), and phase 1 Pisgah lava (1).

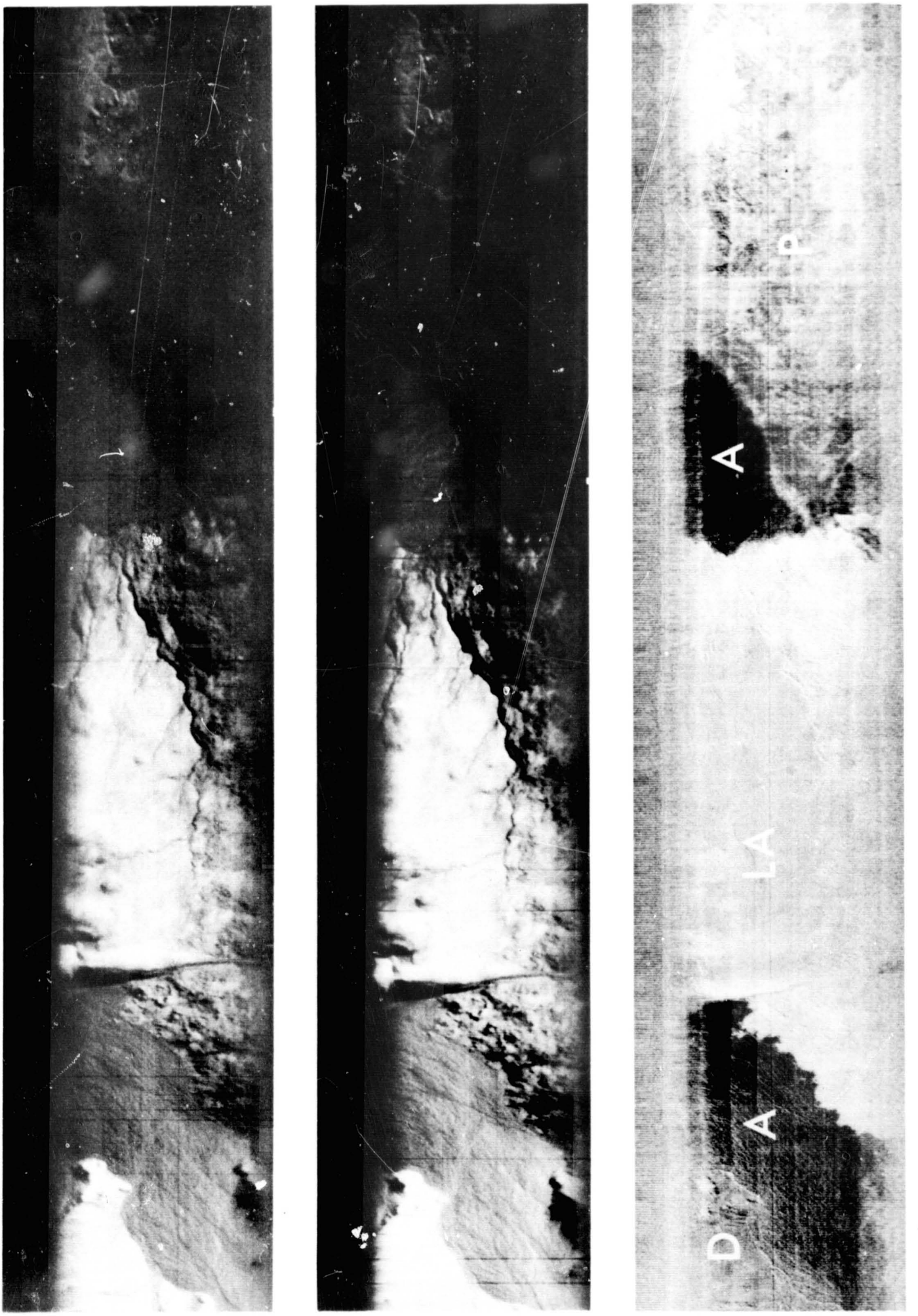

FIGURE 1

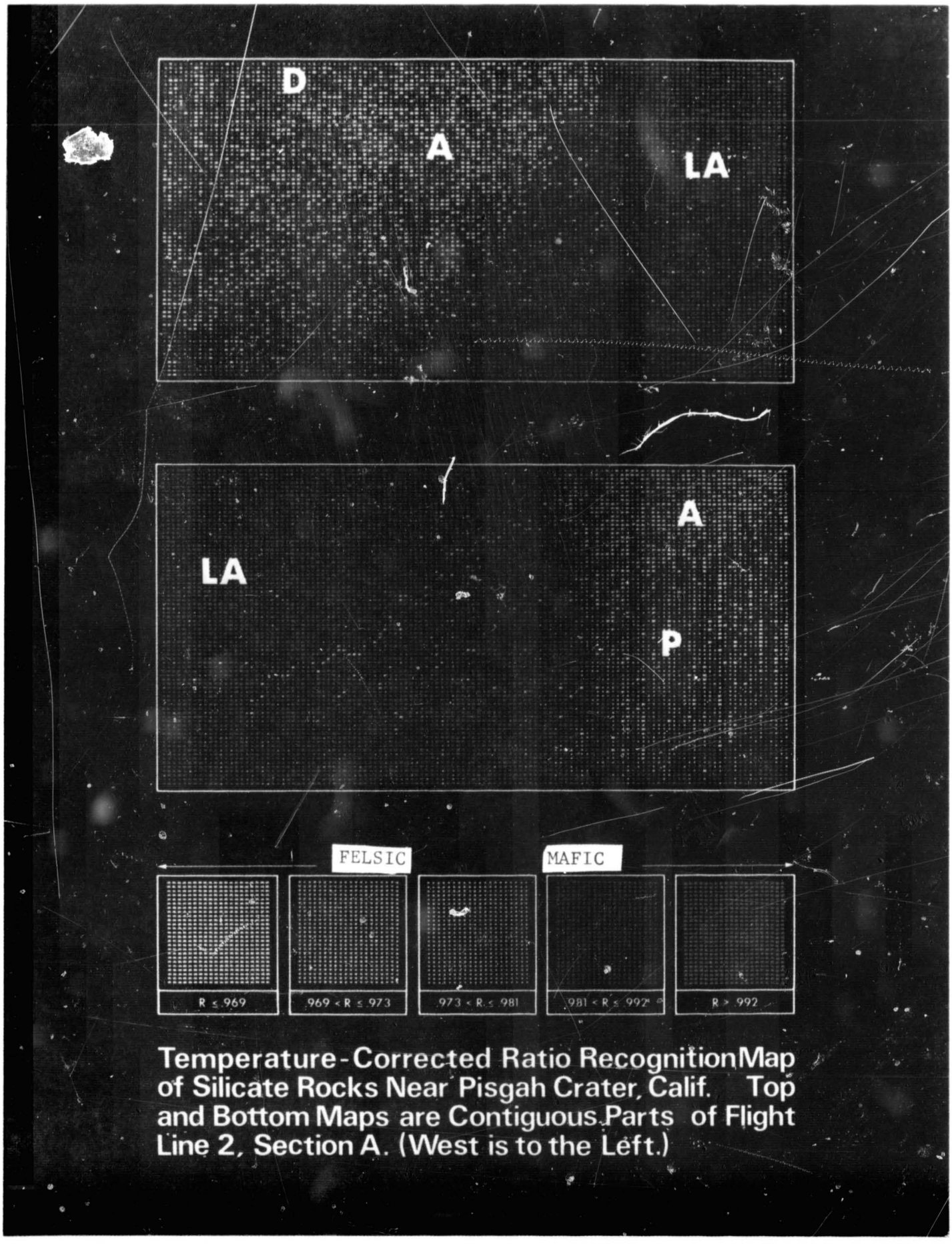

Temperature-Corrected Ratio Recognition Map of Silicate Rocks Near Pisgah Crater, Calif. Top and Bottom Maps are Contiguous Parts of Flight Line 2, Section A. (West is to the Left.)

FIGURE 2

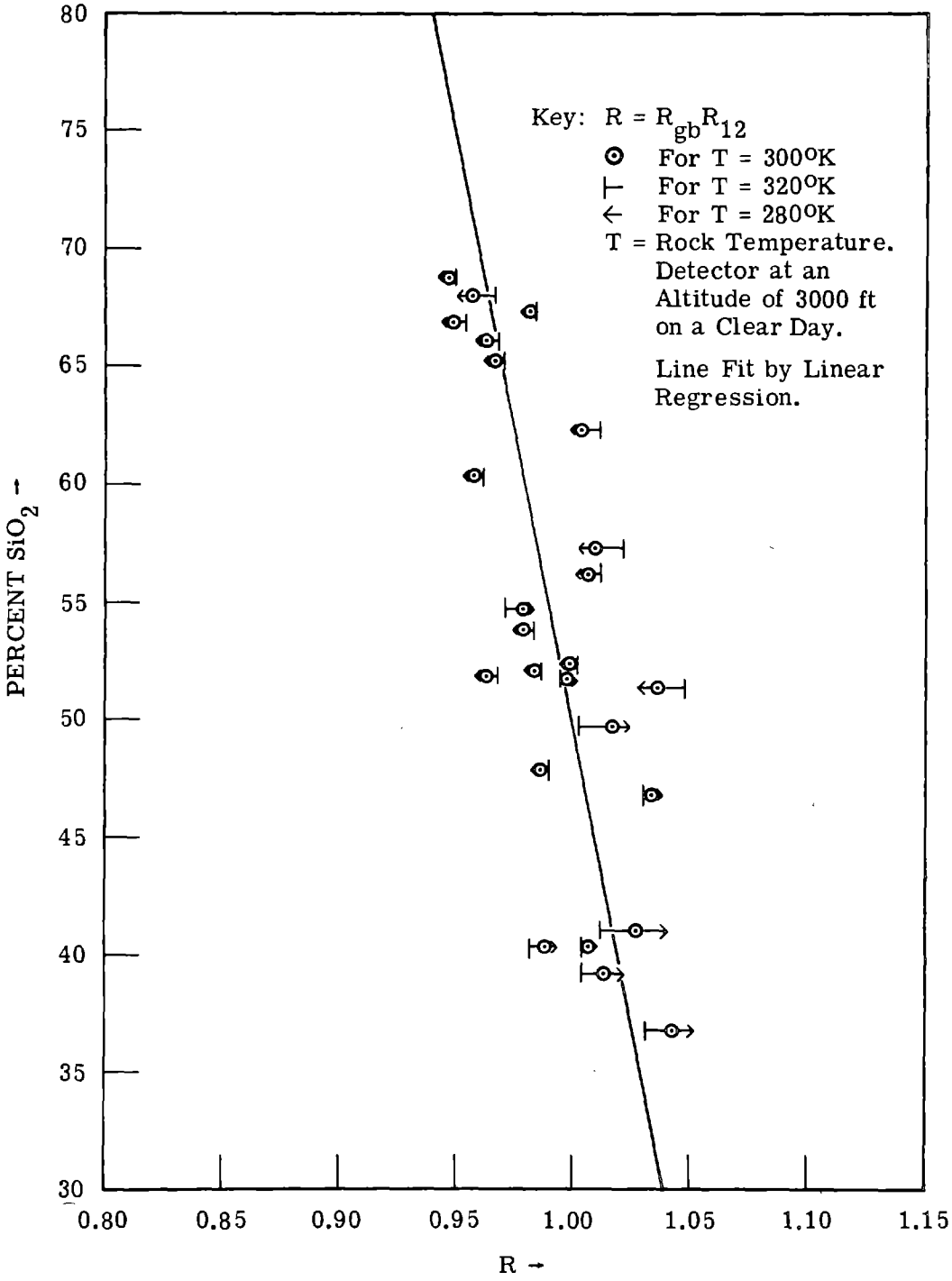

FIGURE 3. TEMPERATURE-CORRECTED RATIO VERSUS PERCENT SiO_2

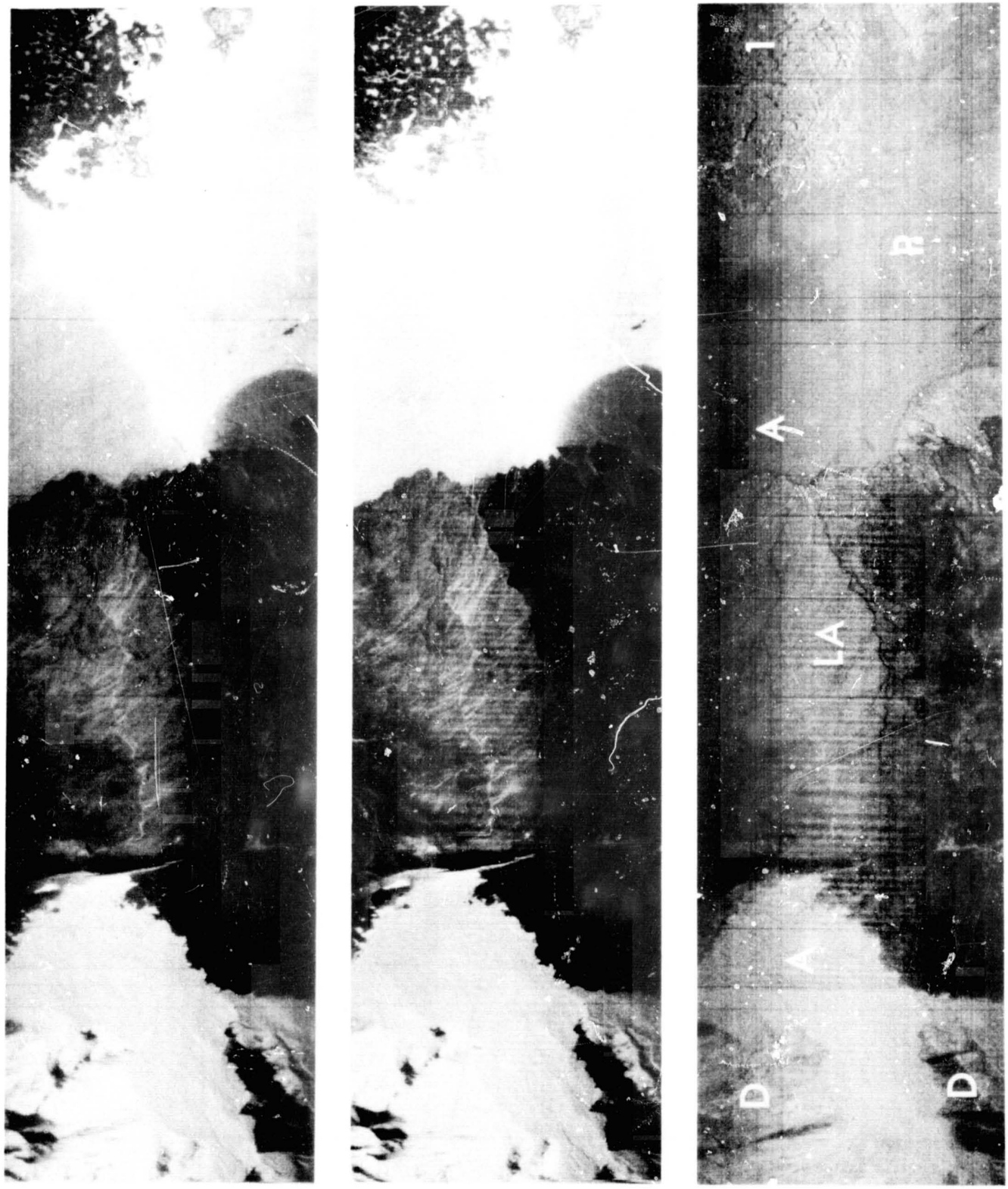

FIGURE 4